Earth Sciences Scholarship

Earth Sciences

2-27-2003

Effect of sulfate aerosol on tropospheric NOx and ozone budgets: Model simulations and TOPSE evidence

Xuexi Tie
NCAR

L K. Emmons
National Center for Atmospheric Research

Larry Horowitz
NOAA

Guy Brasseur
Max-Planck Institute of Meteorology

Brian Ridley
NCAR

See next page for additional authors

Recommended Citation

Authors

Xuexi Tie, L K. Emmons, Larry Horowitz, Guy Brasseur, Brian Ridley, Elliot Atlas, Craig Stround, Peter Hess, Andrzej Klonecki, Sasha Madronich, R. Talbot, and Jack E. Dibb

Effect of sulfate aerosol on tropospheric NO$_x$ and ozone budgets: Model simulations and TOPSE evidence

Xuexi Tie,[1] Louisa Emmons,[1] Larry Horowitz,[2] Guy Brasseur,[3] Brian Ridley,[1] Elliot Atlas,[1] Craig Stround,[1] Peter Hess,[1] Andrzej Klonecki,[1] Sasha Madronich,[1] Robert Talbot,[4] and Jack Dibb[4]

[1] The distributions of NO$_x$ and O$_3$ are analyzed during TOPSE (Tropospheric Ozone Production about the Spring Equinox). In this study these data are compared with the calculations of a global chemical/transport model (Model for OZone And Related chemical Tracers (MOZART)). Specifically, the effect that hydrolysis of N$_2$O$_5$ on sulfate aerosols has on tropospheric NO$_x$ and O$_3$ budgets is studied. The results show that without this heterogeneous reaction, the model significantly overestimates NO$_x$ concentrations at high latitudes of the Northern Hemisphere (NH) in winter and spring in comparison to the observations during TOPSE; with this reaction, modeled NO$_x$ concentrations are close to the measured values. This comparison provides evidence that the hydrolysis of N$_2$O$_5$ on sulfate aerosol plays an important role in controlling the tropospheric NO$_x$ and O$_3$ budgets. The calculated reduction of NO$_x$ attributed to this reaction is 80 to 90% in winter at high latitudes over North America. Because of the reduction of NO$_x$, O$_3$ concentrations are also decreased. The maximum O$_3$ reduction occurs in spring although the maximum NO$_x$ reduction occurs in winter when photochemical O$_3$ production is relatively low. The uncertainties related to uptake coefficient and aerosol loading in the model is analyzed. The analysis indicates that the changes in NO$_x$ due to these uncertainties are much smaller than the impact of hydrolysis of N$_2$O$_5$ on sulfate aerosol. The effect that hydrolysis of N$_2$O$_5$ on global NO$_x$ and O$_3$ budgets are also assessed by the model. The results suggest that in the Northern Hemisphere, the average NO$_x$ budget decreases 50% due to this reaction in winter and 5% in summer. The average O$_3$ budget is reduced by 8% in winter and 6% in summer. In the Southern Hemisphere (SH), the sulfate aerosol loading is significantly smaller than in the Northern Hemisphere. As a result, sulfate aerosol has little impact on NO$_x$ and O$_3$ budgets of the Southern Hemisphere. *INDEX TERMS:* 0305 Atmospheric Composition and Structure: Aerosols and particles (0345, 4801); 0365 Atmospheric Composition and Structure: Troposphere—composition and chemistry; 0368 Atmospheric Composition and Structure: Troposphere—constituent transport and chemistry; *KEYWORDS:* tropospheric aerosol, NO$_x$, ozone

1. Introduction

[2] Sulfate aerosol plays important roles in the Earth's radiation balance. It can directly affect the Earth's radiative budget by scattering radiation. It also can indirectly influence the radiation budget through its participation in cloud formation. Sulfate aerosol can also have strong interactions with oxidants in the atmosphere through heterogeneous surface reactions. It is well known that the hydrolysis of N$_2$O$_5$ on sulfate aerosol impacts stratospheric nitrogen partitioning by converting reactive nitrogen oxide (NO$_x$ = NO + NO$_2$) to a longer-lived nitrogen reservoir species, HNO$_3$. Including this reaction, models produce remarkably better agreement between calculated and observed NO$_x$ concentrations in the stratosphere [*Fahey et al.*, 1993]. Reduction of NO$_x$ due to volcanic eruption is clearly detected by ground based NO$_2$ measurements [*Johnston et al.*, 1992; *Koike et al.*, 1994]. Modeling calculations also show evidence that NO$_x$ concentrations are significantly reduced when sulfate aerosol concentrations are greatly enhanced after large volcanic eruptions [*Hofman and Solomon*, 1989; *Rodriguez et al.*, 1991; *Brasseur and Granier*, 1992; *Pitari and Rizi*, 1993; *Bekki and Pyle*, 1994; *Tie et al.*, 1994].

[3] In the troposphere and stratosphere, NO$_x$ is closely related to O$_3$ chemistry via two separate processes. In the

---

[1]National Center for Atmospheric Research, Boulder, Colorado, USA.
[2]NOAA/GFDL, Princeton University, Princeton, New Jersey, USA.
[3]Max-Planck Institute of Meteorology, Hamburg, Germany.
[4]Institute for the Study of Earth, Oceans, and Space, University of New Hampshire, Durham, New Hampshire, USA.

troposphere, O$_3$ is produced photochemically in the cycling of NO to NO$_2$, which is facilitated by peroxyl radicals formed during oxidation of carbon monoxide, methane, and other volatile organic compounds (VOCs); while in the stratosphere, O$_3$ is catalytically destroyed by NO$_x$. Nitrogen oxides are also intricately linked to the hydroxyl radical, OH, another key atmospheric oxidizing species. The reaction between NO$_2$ and OH leads to the formation of relatively stable nitric acid (HNO$_3$), which can be removed from the atmosphere by wet and dry deposition and hence provides an important source of nitrogen for the biosphere. NO$_x$ also affects the production of OH. When NO$_x$ changes from low to moderate levels, the oxidation of hydrocarbons results in the production of O$_3$. Enhanced O$_3$ results in greater production of OH via O$_3$ photolysis. Also, since O$_3$ strongly absorbs the Earth's infrared radiation, knowledge of the regional and global NO$_x$ distribution is important for climate studies.

[4] Several studies suggest that hydrolysis of N$_2$O$_5$ on sulfate aerosol can play an important role in tropospheric chemistry. Model studies by *Dentener and Crutzen* [1993] and *Tie et al.* [2001] show that this heterogeneous reaction can reduce the tropospheric NO$_x$ budget up to 50% in the Northern Hemisphere during winter. As a result, O$_3$ concentrations are reduced by 10 to 20% in the Northern Hemisphere. The direct in-situ measurement of the effect of hydrolysis of N$_2$O$_5$ on NO$_x$ and O$_3$ concentrations is difficult because NO$_x$ and O$_3$ concentrations are not only impacted by the hydrolysis, but are also affected by other chemical and physical processes such as gas-phase chemistry and transport. A simultaneous measurement of chemical species (N$_2$O$_5$, NO$_x$, and O$_3$) and sulfate aerosols can provide very useful information in order to verify the model results. However, there have been few observations to compare the global model assessments of the impact of N$_2$O$_5$ hydrolysis on tropospheric chemistry.

[5] In this paper, we compare model results to field observations of NO$_x$, O$_3$, and sulfate aerosol to demonstrate that the hydrolysis of N$_2$O$_5$ on sulfate aerosol has a significant impact on NO$_x$ and O$_3$ budgets in the troposphere, and we will show that observations of NO$_x$ and O$_3$ during TOPSE strongly support this conclusion.

[6] The paper is divided into several sections. Section 2 provides a description of the model assessment of the effect of hydrolysis of N$_2$O$_5$ on sulfate aerosol on global NO$_x$ and ozone budgets, and comparison to the observations during TOPSE. Section 3 discusses the uncertainties in model calculations and their effect on the conclusions, and section 4 gives a summary of this study.

2. Method and Results

2.1. Model Assessment of Global NO$_x$ and O$_3$ Budgets Due to N$_2$O$_5$ Hydrolysis

[7] The NCAR global chemical transport model (MOZART) is used in this study. The model is a comprehensive tropospheric chemical/transport model, calculating the global distribution of 56 gas-phase chemical species. The nitrogen species in the model include NO$_x$, HNO$_3$, N$_2$O$_5$, HNO$_4$, NO$_3$, and PAN (CH$_3$CO$_3$NO$_2$). Currently, HONO is not included in the MOZART model. The detailed model configurations (version 1) are described in *Brasseur*
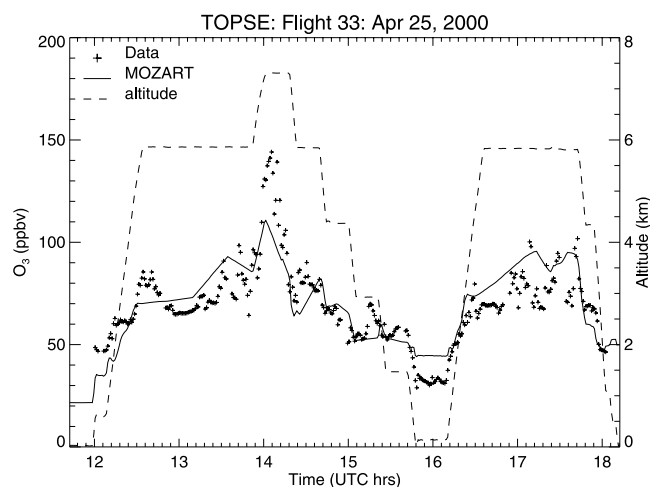

Figure 1. Calculated and measure O$_3$ concentrations during the TOPSE flight 33 (April 25/2000). The solid dots are the calculations, and the solid line is the measurements. The dashed line is the flight altitude. The hydrolysis of N$_2$O$_5$ on sulfate aerosol is included in the model.

et al. [1998]. The calculated climatological distributions of tropospheric chemical species have been validated by comparison to measurements [*Hauglustaine et al.*, 1998]. In this early version of MOZART, the hydrolysis of N$_2$O$_5$ is parameterized according to the method suggested by *Muller and Brasseur* [1995]. The results show that the model calculated tropospheric CO, O$_3$ and NO$_x$ concentrations are generally consistent with the observations, especially in the tropics. The global OH budget is estimated by calculating the CH$_4$ chemical lifetime. The model estimate of CH$_4$ lifetime is about 10 years, which is comparable or slightly higher than previous estimations [*Prinn et al.*, 1987; *Tie et al.*, 1992]. In this study, the chemical and transport schemes are updated from the version used by *Brasseur et al.* [1998]. Heterogeneous reactions of N$_2$O$_5$ on sulfate aerosols are included, with the sulfate aerosol distribution prescribed based on a sulfate aerosol mass distributions. The sulfate area is then calculated from sulfate aerosol mass loading with an assumption that the mean radius of sulfate aerosols is 0.15 μm [*Tie et al.*, 2001]. The kinetic reaction rates are based on laboratory measurement [*Hu and Abbatt*, 1997]. Advection of tracers is performed using the flux-formed semi-Lagrangian advection scheme of *Lin and Rood* [1996]. The deep convection scheme developed by *Zhang and McFarlane* [1995] is included in the model. The detailed description of the updated MOZART is described by L. W. Horowitz, et al. (A global simulation of tropospheric ozone and related tracers: Description and evaluation of MOZART, version 2, manuscript in preparation, 2001). The model can be either driven by ECMWF (European Centre for Medium-Range Weather Forecasts) assimilated wind fields or by NCAR- CCM (Community Climate Model) wind fields. For this work, ECMWF assimilated wind fields for 2000 were used as dynamical inputs in the model. The ECMWF fields have a horizontal resolution of 2 degree by 2 degree and 60 levels to 0.1 mb, so that local synoptical scale transport events can be captured in the model during TOPSE flights. Figure 1 shows an example of

the model calculated O$_3$ during the TOPSE fights. Synoptic events such as stratospheric O$_3$ intrusions are clearly indicated from the model calculations. More detailed analysis is given by L. K. Emmons et al. (The budget of tropospheric ozone during TOPSE from two CTMs, manuscript submitted to *Journal of Geophysical Research,* 2002).

[8] The reaction coefficient of the hydrolysis of N$_2$O$_5$ can be written as [*Schwartz*, 1986];

$$k_{het} = [r/Dg + 4/(c\gamma)]^{-1} A \times 10^8 \qquad (1)$$

Where $c = [8kT/m]^{1/2}$ (cm/s) is the mean molecular speed of the gas at temperature T, A(m^2/cm^3) is the surface area density of the particles, γ is the uptake coefficient, m(gram) is the molecular mass of the gas-phase molecule under consideration, k is the Boltzmann constant, Dg (cm^2/s) is the gas-phase diffusion coefficient and r is the mean radius of the aerosol particles. According to the calculation of *Perry and Green* [1984], Dg is close to 0.1 cm^2/s. To convert the mass into surface area, we assume aerosols are spherical with a mean radius of 0.15 μm according to the observation by *Blake and Kato* [1995]. The sulfate surface area is growth with humidity according to an empirical formula suggested by *Shettle and Fenn* [1979]. According to the analysis of *Dentener and Crutzen* [1993], when $\gamma < 0.1$, the term $4/(c\gamma)$ dominates, and Equation (1) can be written as;

$$k_{het} = (c\gamma)/4 \times A \times 10^8 \qquad (2)$$

[9] The effect of the hydrolysis of N$_2$O$_5$ on sulfate aerosols on NO$_x$ starts with the following gas-phase reactions:

(R-1)   NO$_2$ + O$_3$ → NO$_3$ + O$_2$

(R-2)   NO$_2$ + NO$_3$ + M → N$_2$O$_5$ + M

(R-3)   N$_2$O$_5$ + M → NO$_3$ + NO$_2$ + M
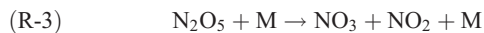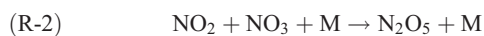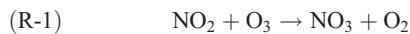
The ratio of the reaction coefficients of R-2 and R-3 determines the amount of N$_2$O$_5$, which is stabilized relative to that which is decomposed. The ratio is strongly temperature dependent. When the temperature is low, N$_2$O$_5$ concentration is high, suggesting that during winter it is more favorable for the formation of N$_2$O$_5$. When N$_2$O$_5$ is available in the atmosphere, hydrolysis of N$_2$O$_5$ on sulfate aerosol takes place, i.e.:

(R-4)   N$_2$O$_5$ + (H$_2$O in sulfate) → 2HNO$_3$(gas-phase)
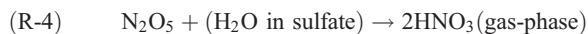
The net result from R-1 to R-4 is to generate a chain pathway that converts NO$_2$ to HNO$_3$. However, this conversion only occurs during nighttime. During daytime, NO$_3$ is quickly destroyed by photo-dissociation, and the reaction of R-2 is slowed. The conversion of NO$_x$ to HNO$_3$ is mainly through the following reaction

(R-5)   OH + NO$_2$ + M → HNO$_3$ + M.

Because the daytime conversion of NO$_2$ to HNO$_3$ is much slower than the nighttime conversion, as indicated in Figure 2,

R-5 has a small effect on the net loss of NO$_2$ when the nighttime loss is included. Figure 2 is a schematic of the conversion of NO$_x$ into HNO$_3$ during nighttime and daytime. During nighttime, the conversion of NO$_x$ into HNO$_3$ is through a series of chain reactions. The numbers in parentheses show the chemical time constants (hours) of the reaction averaged over the NH below 5 km during winter. The reaction with the slowest rate is the rate limiting step in the chain, which determines the net rate of the conversion. In these reactions (R-1 to R-4), the rate-limiting step is R-1 with a chemical time constant of 26 hours. The time constant for hydrolysis of N$_2$O$_5$(R-4) on sulfate is about 2.5 hours (with uptake coefficient $\gamma = 0.1$) which is about 10 times faster than R-1. However, without hydrolysis of N$_2$O$_5$, the conversion of NO$_x$ to HNO$_3$ will be terminated during nighttime. In this case, daytime conversion (R-5) is the only pathway to convert NO$_2$ to HNO$_3$. The chemical time constant of R-5 is about 5 times longer than that during nighttime when hydrolysis of N$_2$O$_5$ on sulfate is considered. This implies that hydrolysis of N$_2$O$_5$ on sulfate provides a very effective conversion of NO$_x$ to HNO$_3$. However, from the above analysis, the following conditions are required for this conversion: (1) sunlight is low (nighttime or polar night), (2) temperature is low, leading to a low decomposition rate of N$_2$O$_5$ by R-3, so that the N$_2$O$_5$ concentration is high, and (3) sulfate aerosol surface areas are relatively high, producing a high rate of hydrolysis of N$_2$O$_5$. Such conditions are often found in the NH at high latitudes in winter. It is noted that including the hydrolysis of N$_2$O$_5$ leads to increase in HNO$_3$. Generally, the calculated HNO$_3$ concentration is overestimated by chemical models [*Chatfield*, 1994; *Jacob et al.*, 1996; *Hauglustaine et al.*, 1998; *Wang et al.*, 1998a, 1998b]. In middle latitudes of the NH, the zonally averaged calculated HNO$_3$/NO$_x$ ratio is about 5 in summer and 5 to 20 in winter in the lower and middle troposphere, which consistent to other calculations [*Chatfield*, 1994; *Jacob et al.*, 1996; *Wang et al.*, 1998a, 1998b]. The problem of the overestimation of HNO3 could be due to several chemical and physical processes. The problem is beyond the scope of this paper, and will not be discussed in this paper.

[10] To provide a global view and to understand the spatial and temporal distributions of the effect of hydrolysis of N$_2$O$_5$ on sulfate aerosol (with an uptake coefficient of 0.1 as a standard calculation) on NO$_x$ and O$_3$ budgets, the model was run with and without R-4. Then the differences between the model runs were analyzed for the impact of R-4 on the global NO$_x$ and O$_3$ distributions in different seasons. Figure 3 shows the changes in NO$_x$ at surface due to including R-4 in December and in June. The results show that hydrolysis of N$_2$O$_5$ on sulfate aerosol has a significant impact on global NO$_x$ distributions. The maximum NO$_x$ reduction due to this reaction occurs at high latitudes in the NH during winter. At latitudes between 50°N and the North Pole, the magnitude of the reduction is about 60 to 90% (corresponding to a few hundred pptv in absolute concentrations), indicating that a significant amount of NO$_x$ is removed by the sulfate aerosol in and near polar night region. During summer, reduction of NO$_x$ due to this reaction is smaller (less than 20 percent in most of the globe) than during winter. In the Southern Hemisphere, the changes in NO$_x$ are small because most anthropogenic sulfur emission occurs in the NH. During summer the effect
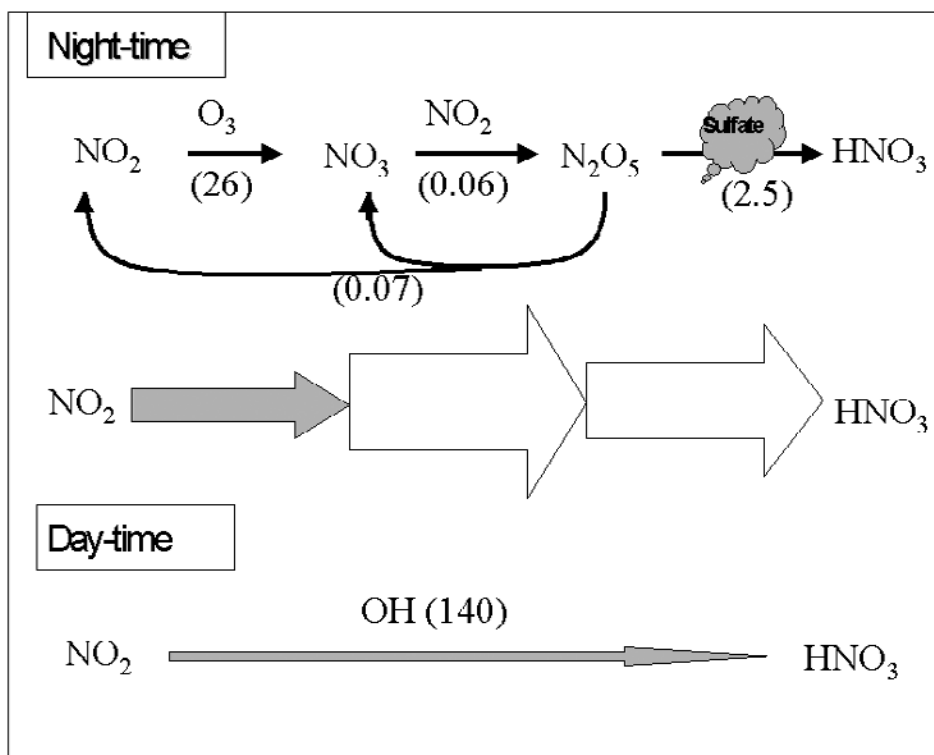
Figure 2. A schematic of the conversion of NO$_x$ into HNO$_3$ during nighttime and daytime. The numbers in parentheses are the chemical reaction time constants (hours) averaged over the NH below 5 km during winter. The size of the arrows is proportional to the reaction rates.

of R-4 on NO$_x$ concentrations in the SH is negligible. Some regional characters are also noticed. In the polluted regions over North America (in the US and southern Canada), despite the largest changes in absolute concentrations in NO$_x$ (not show), the percentage changes are smaller than the regions in high latitudes near the North Pole because the background NO$_x$ concentrations are very high in the US and southern Canada. In the Southern Hemispheric winter there is a 20 to 30% change in NO$_x$ at 60°S where large amounts of dimethyl sulfide (DMS) are released, and oxidized to form sulfate aerosols [*Tie et al.*, 2001].

[11] O$_3$ is produced in the troposphere by oxidation of hydrocarbons and CO, catalyzed by HO$_x$ and NO$_x$. As a result, the large reduction in NO$_x$ due to hydrolysis of N$_2$O$_5$ on sulfate aerosol will lead to changes in tropospheric O$_3$ concentrations. Figure 4 shows the calculated surface O$_3$ reductions in winter (December) and in summer (June) due to R-4. It shows that O$_3$ concentrations are significantly reduced in the NH. The maximum O$_3$ reduction (20%) occurs at midlatitudes during winter. The O$_3$ reduction at high latitudes is smaller than at midlatitudes even though the decrease in NO$_x$ at high latitudes is largest. This is a result of OH concentrations being lower at high latitudes than at midlatitudes during winter, leading to a lower ozone production in this region. During summer at high latitudes in the NH, although the NO$_x$ reduction is much smaller than during winter, the reduction of O$_3$ concentrations occurs with a similar magnitude (10%) compared to that during winter. This is a result of the strong seasonality of OH, i.e., mean OH in the NH is normally 3 times higher in summer

than in winter [*Tie et al.*, 1992]. Because O$_3$ production in the troposphere depends on the rate of the reactions of OH with CO, CH$_4$, and VOC as well as the rate of NO$_2$ photolysis, the combination of the higher OH concentrations and stronger NO$_2$ photolysis produces a relative higher O$_3$ reduction in this region due to the impact of hydrolysis of N$_2$O$_5$. In the SH, the reduction in O$_3$ concentrations is not significant. Some regional characters are also noticed. In some polluted regions such as in the eastern US, the NO$_x$ concentrations are very high. The reduction of NO$_x$ due to hydrolysis of N$_2$O$_5$ produces relatively smaller changes in O$_3$ due to the fact that the NO$_x$ and O$_3$ relationship is nonlinearly correlated and complicated as suggested by *Sillman et al.* [1990].

[12] Figures 5a and 5b show the zonally averaged changes in NO$_x$, O$_3$, and OH in June and December due to R-4, in percent and in mixing ratio respectively. The upper panels of Figure 5a show the percentage changes in NO$_x$. It shows that NO$_x$ reduction has very strong latitudinal and altitudinal variations. The NO$_x$ reduction is well confined in the NH, with a maximum of 80 to 90% reduction at 60°N in the lower troposphere in December, and a very sharp gradient in the reduction takes place between 50°N and the equator. In the tropical region, the reduction is negligible. In the SH, the maximum reduction is about 10% in high latitudes in June as result of the high DMS emission in this region. The altitudinal distribution of the reduction reveals that the reduction is highest in the lower troposphere, and it rapidly decreases with altitude. At 15 km, the reduction decreases to 20%, suggesting that the greatest
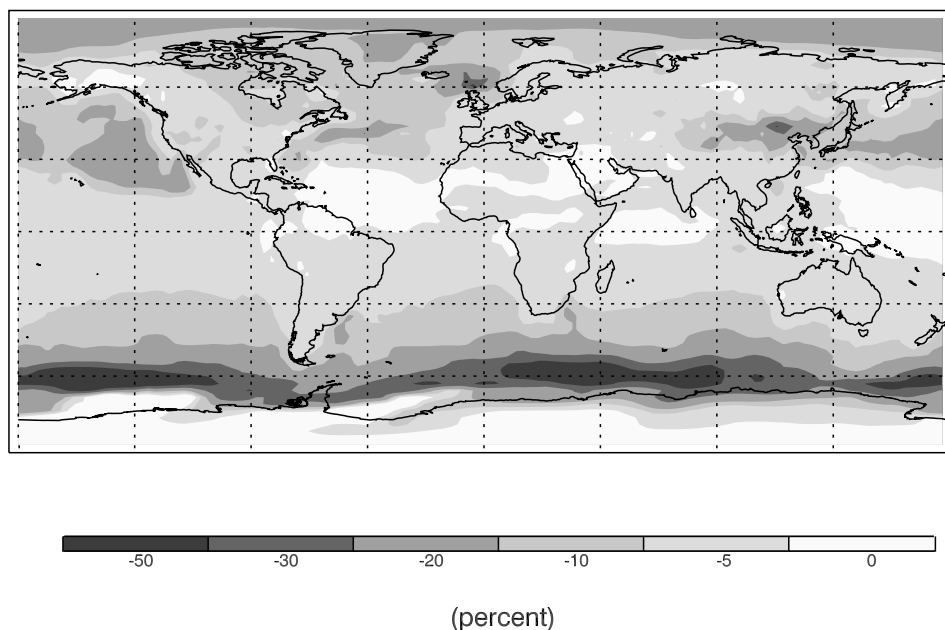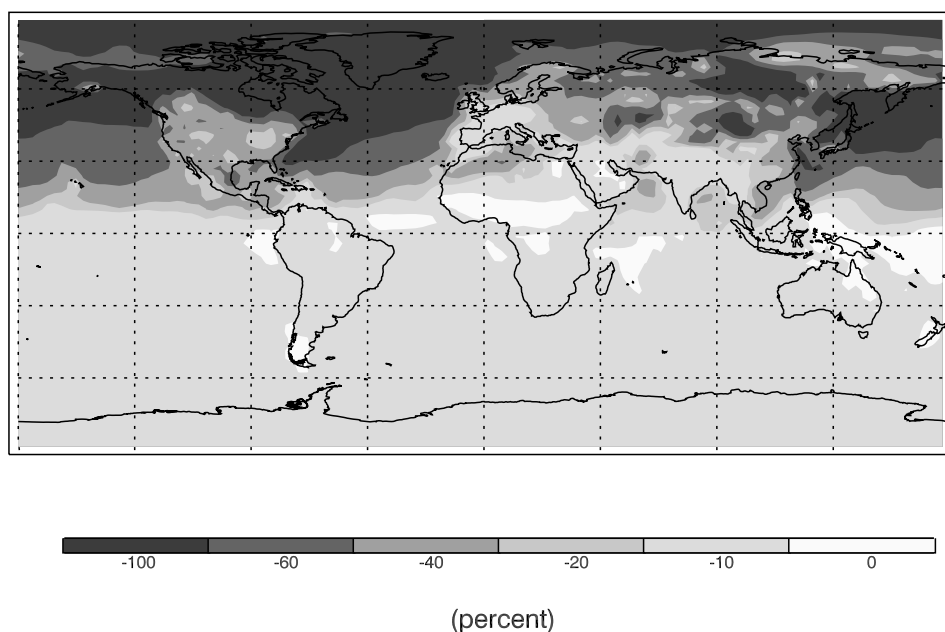
NOx reduction in June

NOx Reduction in Dec.

Figure 3. Calculated changes (percent) due to hydrolysis of N$_2$O$_5$ on sulfate aerosol ($\gamma = 0.1$) for NO$_x$ concentrations at the surface in December (top) and in June (bottom).

NO$_x$ reduction is well confined in the lower troposphere, consistent with the location of most of the sulfate aerosols [*Tie et al.*, 2001]. We note that the maximum absolute changes in the NH are near the surface (see Figure 5b). However, the percentage change is located between 2 and 6 km (see Figure 5a) due to the fact that the background values are the highest at the surface.

[13] The middle panels of Figure 5a show the changes of O$_3$. The O$_3$ reduction is limited to the NH, with a maximum of 10% reduction between 50°N and the North Pole in December, and 8 to 10% in June. A very sharp latitudinal gradient of the reduction takes place between midlatitudes and the equator. Except in this transition region, the reduction is relatively small in the SH. Between 50°N and the North Pole the chemical lifetime of O$_3$ is relatively long, and O$_3$ concentrations in these regions are well mixed. The reduction of O$_3$ is also confined to the lower to middle troposphere, with a maximum reduction of
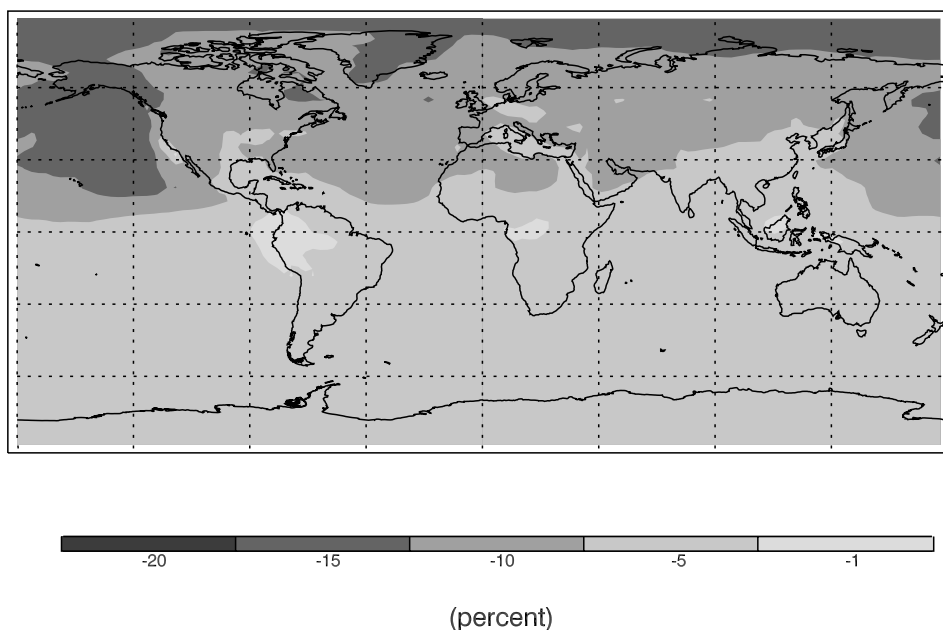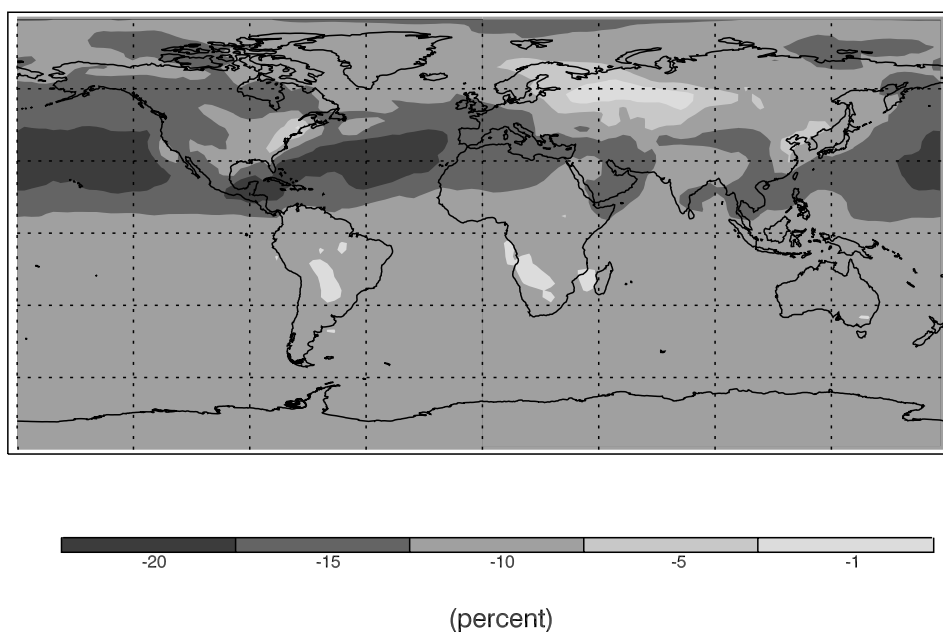
O3 reduction in June

(percent)

O3 Reduction in Dec.

(percent)

Figure 4.   Same as Figure 3 except for O$_3$.

10% below 6 km, decreasing with altitude to a reduction of 2% above 10 km.

[14] The lower panels of Figure 5a show the percentage changes of OH. The reduction of OH is correlated with the O$_3$ reduction, suggesting that the reduction of O$_3$ concentrations produces the reduction of OH concentrations. In the NH, the largest OH reduction is located in 50°N in the lower troposphere in December with a maximum of 30 to 40% reduction. Despite the largest reduction of the absolute changes in June (see Figure 5b), the percentage changes

in OH are smaller in June than in December because the background values are higher in summer than in winter. In the SH, the reduction of OH is very small. The reduction of OH is also confined to the lower to middle troposphere. Above 10km the reduction of OH is very small.

[15] Figure 6 shows seasonal and latitudinal variations of the reduction of column NO$_x$ and O$_3$ due to R-4. A strong seasonal variation is shown in NO$_x$ and O$_3$ reduction, especially at middle and high latitudes in the NH. However, there is about a 2−3 month lag between the maximum
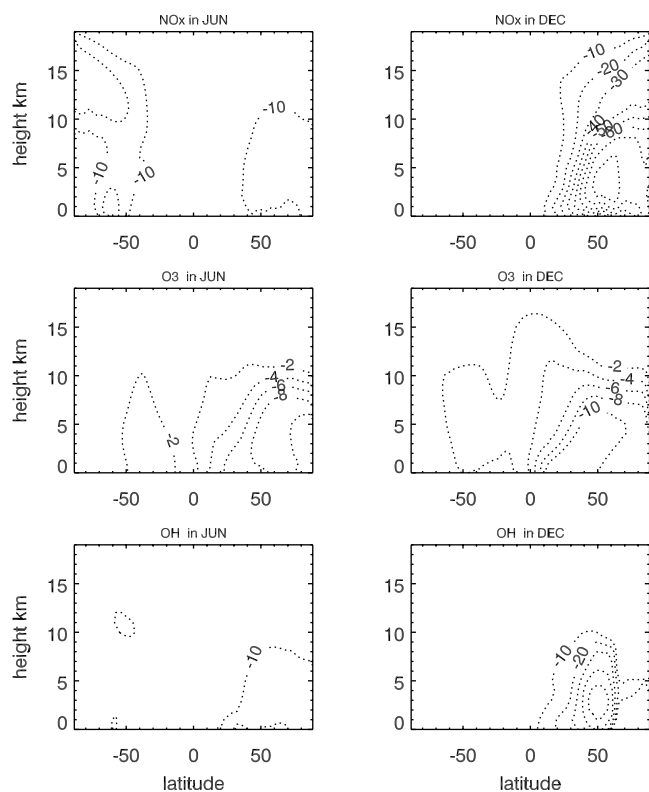
Figure 5a. Calculated zonally averaged changes (%) due to hydrolysis of N$_2$O$_5$ on sulfate aerosols for NO$_x$ (upper panels), O$_3$ (middle panels), and OH (lower panels) in June and December.
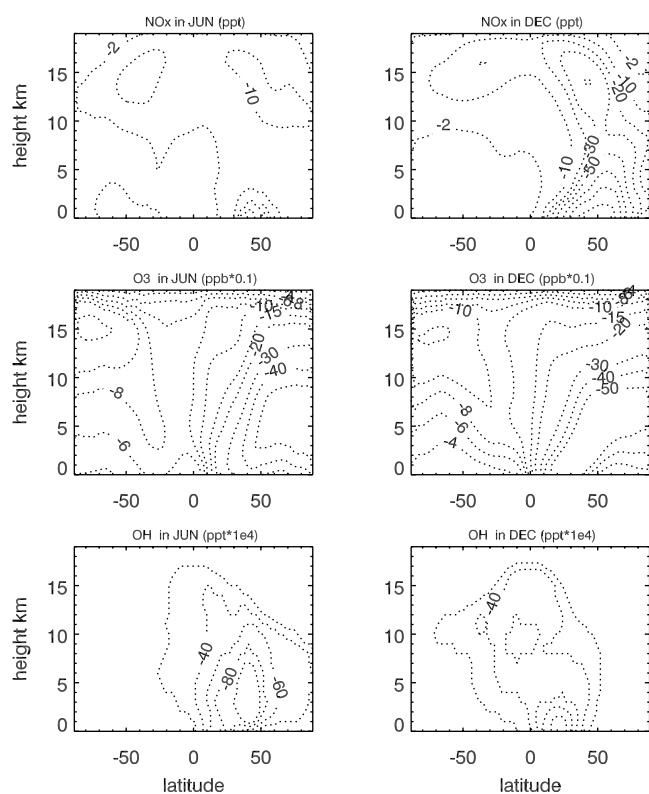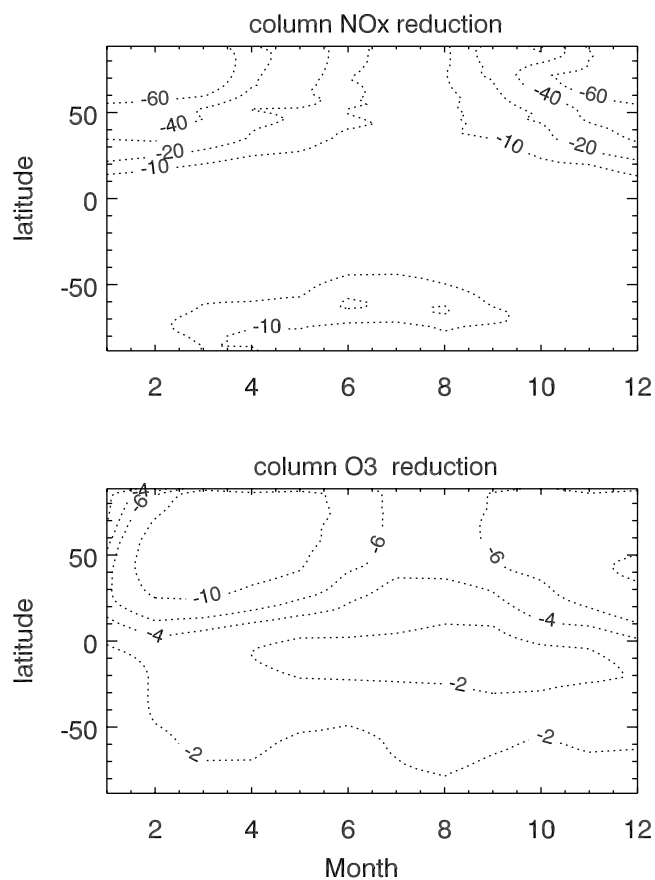

Figure 6. Calculated latitudinal-seasonal reductions in tropospheric column NO$_x$ (top) and O$_3$ (bottom) due to hydrolysis of N$_2$O$_5$ on sulfate aerosol.

Figure 5b. Same as Figure 5a except for changes in mixing ratio.

reduction of O$_3$ and NO$_x$. This is because the maximum NO$_x$ reduction occurs in winter when OH is low. Because OH is a key species for catalytically producing O$_3$, the low OH concentrations in winter have little impact on O$_3$ concentrations even though the NO$_x$ reduction is at a maximum. In early spring, however, the reduction of NO$_x$ is still high, and OH concentrations increase, leading to a maximum in O$_3$ reduction. In the northern high latitude, the reduction of NO$_x$ is at a maximum between November and March with 60% reduction, and is at a minimum in August with less than 10% reduction. The reduction of O$_3$ is at a maximum between February and May with 10% reduction, and is at a minimum in August with less than 6% reduction.

[16] To better understand the spatial and temporal changes of NO$_x$ due to hydrolysis of N$_2$O$_5$, Figure 7 shows the zonally averaged time constant to convert NO$_x$ to HNO$_3$ due to R-5, R-4, and R-1 in June and December. It shows that the rate of OH reacting with NO$_2$ (R-5 in upper panels) is higher in the tropics than in high latitudes, and is higher in summer than in winter. The rate of hydrolysis of N$_2$O$_5$ (R-4 in middle panels) is higher in the NH than in the SH with a maximum in northern middle latitudes of the lower troposphere due to higher sulfate aerosol concentrations. However, the seasonal variability of R-4 is relatively small. The rate of NO$_2$ reacting with O$_3$ (R-1 in lower panels) is also higher in the NH than in the SH with a maximum in northern middle latitudes of the lower troposphere due to
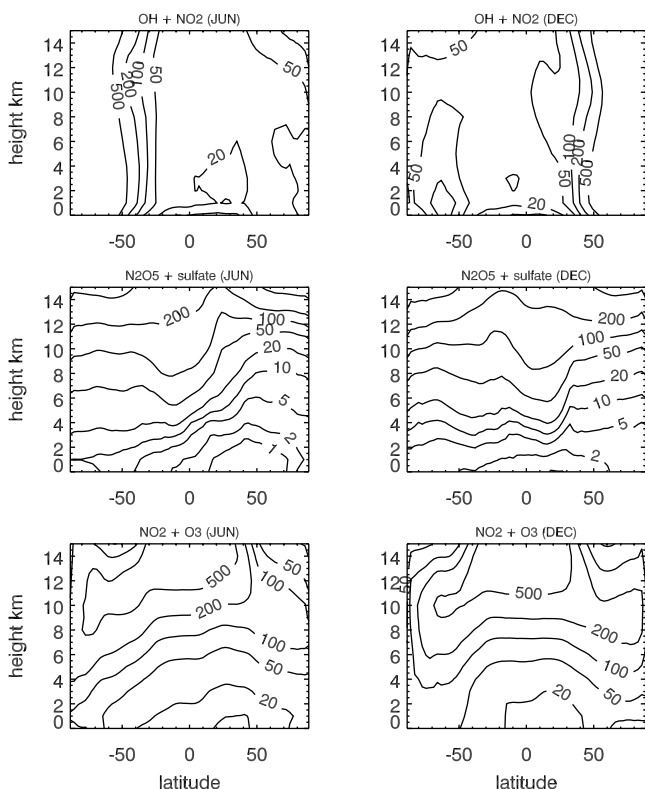
Figure 7. Calculated zonally-averaged chemical time constants of NO$_x$ (hours) due to the chemical reaction of OH + NO$_2$ (upper panels), the hydrolysis of N$_2$O$_5$ on sulfate aerosol (middle panels), and the chemical reaction of NO$_2$ + O$_3$ in June and December.

higher O$_3$ concentrations. Among the reactions, the reaction R-1 is slower than the reaction R-4, indicating that the reaction R-1 is the rate limiting reaction to destroy NO$_2$ due to hydrolysis of N$_2$O$_5$. Comparing the time constants of R-1 and R-5, we see that the hydrolysis provides a fast NO$_x$ chemical destruction in high latitudes during winter in the lower and middle troposphere, especially at high latitudes during winter. However, in the tropics, the reaction of R-1 is normally slower than the reaction R-5. Thus, the hydrolysis plays an insignificant role in destroying NO$_x$ in the tropics.

[17] To provide a hemispheric view of the effect of hydrolysis of N$_2$O$_5$ on sulfate aerosol on NO$_x$ and O$_3$ budgets, we calculate the average changes in NO$_x$ and O$_3$ in the Northern and the Southern Hemispheres during winter and summer (see Figure 8). Figure 8 show that the globally averaged reduction of NO$_x$ has a very strong seasonal variation, with a reduction of 38 and 6% in December and June, respectively. More of the reduction occurs in the NH than in the SH. In the NH, the reduction of NO$_x$ is 47 and 7% during winter and summer, respectively. While in the SH, the reduction of NO$_x$ is 3 and 5% during December and June, respectively. Despite the strong seasonal variation of the reduction of NO$_x$, the globally averaged reduction of O$_3$ has a weak seasonal variation, with 6 and 4% during December and June, respectively. However, in December the O$_3$ reduction shows a large hemispheric asymmetry, with 8 and 2% in the NH and the SH, respectively. We also note that at the present, the model

tends to overestimated HNO$_3$ concentrations, and adding the hydrolysis of N$_2$O$_5$ tend to further increase in HNO$_3$ concentrations. Because the overestimation of the HNO$_3$ is often found by other chemical models [*Chatfield*, 1994; *Wang et al.*, 1998], there are may be some chemical and physical processes which are mistreated in models.

2.2. Comparison to the Results During TOPSE

[18] The TOPSE experiment took place from February to May 2000 in a series of 7 round trip missions from Colorado to northern latitudes [*Atlas et al.*, 2002]. The experiment covered a latitude range from 40°N to near the North Pole, and from 30 to 8000 meters in altitude. The experiment measured O$_3$, NO$_x$, sulfate aerosol and other trace gases which provides a unique characterization of the temporal and spatial distribution of these species to evaluate the effect of hydrolysis of N$_2$O$_5$ on sulfate aerosol on NO$_x$ and O$_3$ concentrations in the free troposphere. Furthermore, the measurements are located in the region where the model indicates the hydrolysis of N$_2$O$_5$ will have the maximum impact on NO$_x$ and O$_3$.

[19] To compare the model results and observations, the model results were interpolated to the TOPSE flight tracks. Averages for each of the 7 missions were then computed for
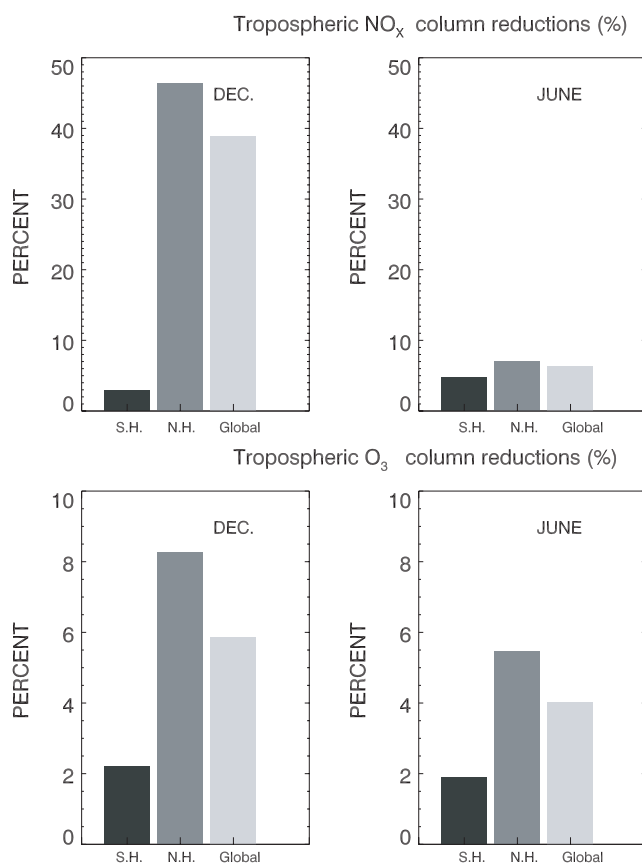

Figure 8. Calculated reductions in NO$_x$ (top) and O$_3$ (bottom) budgets due to hydrolysis of N$_2$O$_5$ on sulfate aerosol in December and in June, respectively. The black bars are the averaged reductions in the SH; the light-black bars are the averaged reductions in the NH; and the gray bars are the averaged reductions for the globe.
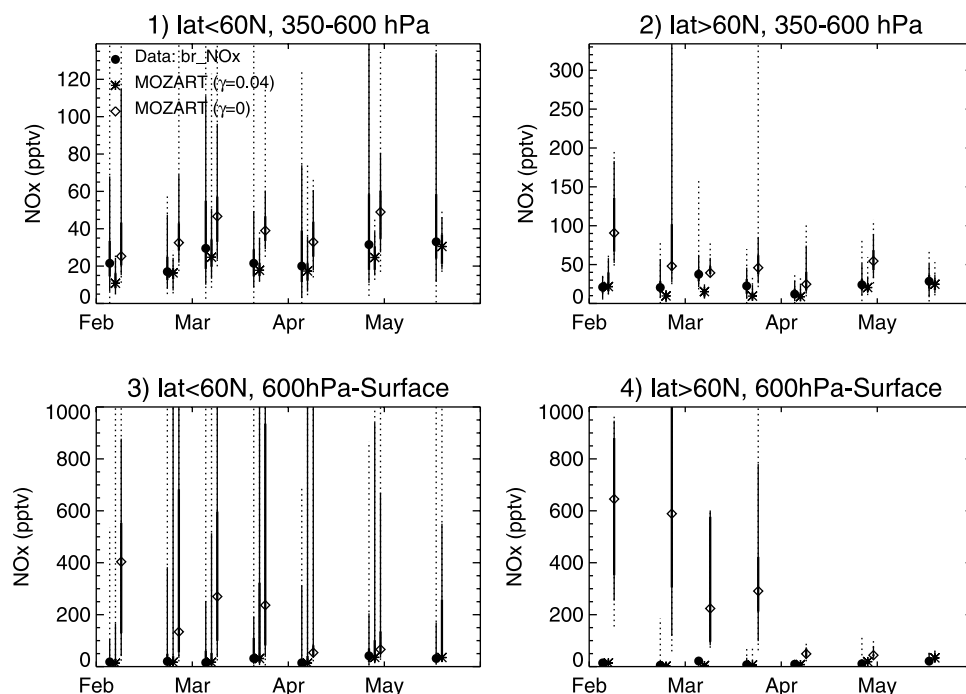
Figure 9a. Comparison of the calculated to the observed NO$_x$ concentrations (pptv) during TOPSE in the following 4 different regions; (1) latitudes <60°N between surface and 600 hPa, (2) latitudes >60°N between surface and 600 hPa, (3) latitudes <60°N between 600 and 300 hPa, and (4) latitudes >60°N between 600 and 300 hPa. The data are averaged for each flight. The black dots are the measured NO$_x$ concentrations; the asterisks are the calculated values with hydrolysis of N$_2$O$_5$ on sulfate aerosol (γ = 0.04); and the diamonds are the calculated values without hydrolysis of N$_2$O$_5$ on sulfate aerosol. The symbols indicate the median values, with thick lines between 25% and 75% of the data, thin lines 5% and 95% and dashed lines between extrema.

observations and model results. The data were divided into the following four regions: (1) latitudes <60°N between 600 and 300 hPa, (2) latitudes >60°N between 600 and 300 hPa, (3) latitudes <60°N between surface and 600 hPa, and (4) latitudes >60°N between surface and 600 hPa. Comparison of the 2 model runs with and without N$_2$O$_5$ hydrolysis and observations (Figure 9a) shows that there is clear evidence that hydrolysis of N$_2$O$_5$ has an important effect on NO$_x$ concentrations during TOPSE. With the hydrolysis of N$_2$O$_5$, the calculated NO$_x$ concentrations are generally consistent with the measured values. However, without hydrolysis of N$_2$O$_5$, the model calculation significantly overestimates observed NO$_x$ concentrations, especially in region 4 in winter (600 pptv by the model via 20 pptv by the measurement). Furthermore, discrepancies between measured and modeled NO$_x$ concentrations have some interesting spatial and seasonal characteristics. For example, in the regions where sulfate aerosol is high (at lower altitudes, in regions 1 and 2), the discrepancies are higher than the regions where sulfate aerosol is low (at higher altitudes, in regions 3 and 4). There is also a strong seasonal variation in which the overestimation of observed NO$_x$ reaches a maximum during winter and early spring, and then significantly decreases during late spring. These spatial and seasonal variabilities are consistent with the model assessment shown in section 2.1. Figure 9b shows the calculated ratio of NO$_x$/NO$_y$ during the TOPSE flights with and without hydrolysis of N$_2$O$_5$ along

with the observed ratio. Because the model is generally overestimated NO$_y$, the calculated ratio has a systemic bias and tend to be lower than the observed ratio. A sensitivity study (not shown) suggests that increase the washout of HNO$_3$ can significantly reduce the concentrations of NO$_y$. With the hydrolysis, the calculated NO$_x$/NO$_y$ ratio is generally overestimated by a factor of 2–10 in comparison to the TOPSE observation. However, without hydrolysis of N$_2$O$_5$, the calculated NO$_x$/NO$_y$ ratio is very high in the lower troposphere during winter when hydrolysis of N$_2$O$_5$ plays an important role in controlling NOx concentrations, suggesting that despite the bias of the lower NO$_x$/NO$_y$ ratio in the calculation, the calculated NO$_x$ concentration is still too high in comparison to the TOPSE observation. In the upper troposphere, however, the effect of hydrolysis is small. The change of the ratio of NO$_x$/NO$_y$ due to the hydrolysis varies within the range of the calculated bias, showing even somewhat improvements in the calculated NO$_x$/NO$_y$ ratio. In these regions (northern middle to high latitudes in the upper troposphere), we cannot see the improvement in modeled NO$_x$ concentrations and NO$_x$/NO$_y$ ratio with hydrolysis of N$_2$O$_5$ before a further improvement of modeled NO$_x$/NO$_y$ ratio is made.

[20] During TOPSE the observed O$_3$ concentrations also show evidence that hydrolysis of N$_2$O$_5$ has an important effect on O$_3$ concentrations in spring. Figure 10 shows that the simulated O$_3$ concentrations are generally in agreement
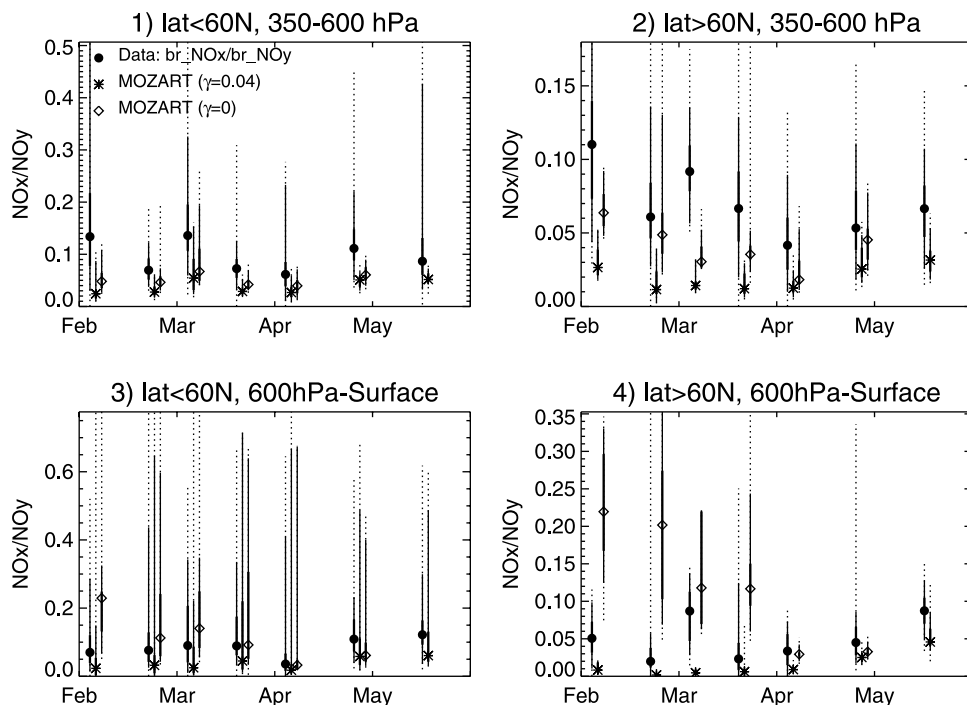
Figure 9b. Same as Figure 9a except for NO$_x$/NO$_y$.

with the observed O$_3$ concentrations when R-4 is included. However, a large discrepancy is found between the measurement and model calculation when R-4 is not included. The discrepancy has a very strong seasonal variability. For example, O$_3$ is significantly overestimated in the lower troposphere in spring with a maximum discrepancy of 40 ppbv. In winter, however, the discrepancies are very small (less than 10 ppbv). The seasonality of the discrep-

ancy is consistent with the model assessment shown in section 2.1. The cause of this seasonal variation is discussed in section 2.1. The statistics of the difference between the modeled O$_3$ and the observed O$_3$ during TOPSE is ranged from +1% to −6% (Emmons et al., submitted manuscript, 2002). Thus, the calculated large O$_3$ discrepancy (20 ppbv) without hydrolysis of N$_2$O$_5$ suggests that the overestimated O$_3$ is mainly due to the hydrolysis.
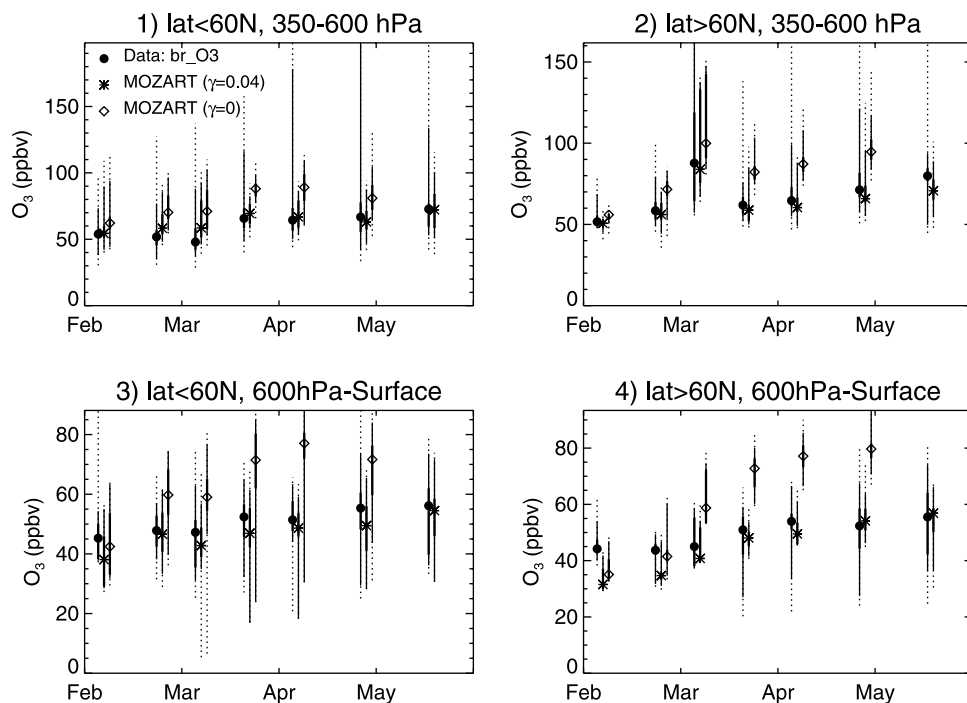

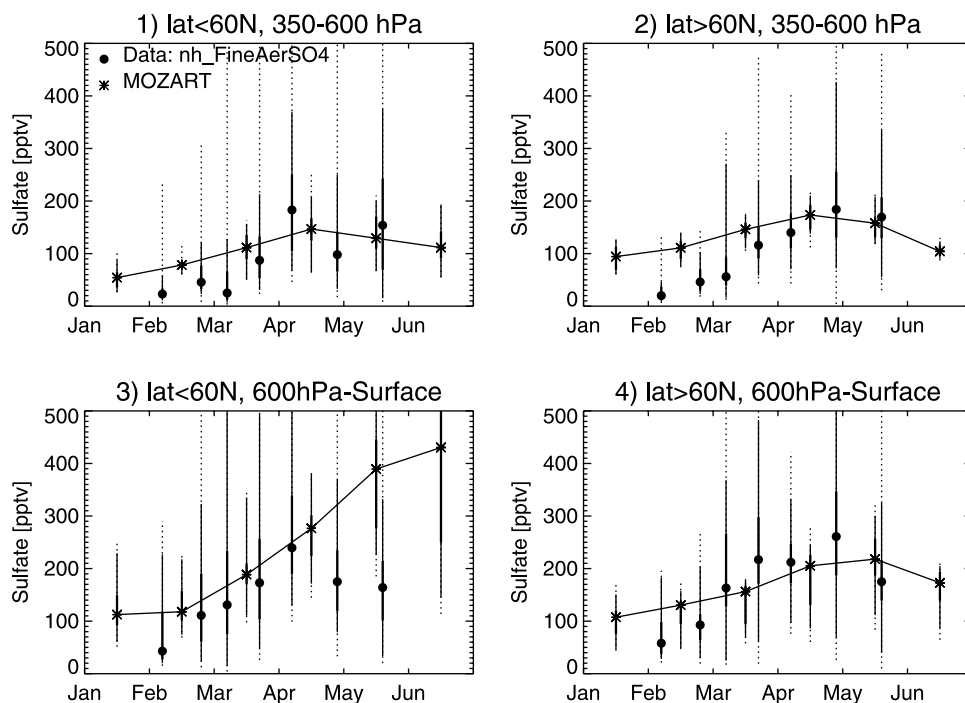**Figure 10.** Same as Figure 9a except for O$_3$.

Figure 11. Comparison of the calculated to the observed sulfate aerosol concentrations (pptv) during TOPSE in the following 4 different regions as in Figure 7. The black dots are the measured sulfate aerosol concentrations, and the asterisks with solid line are the calculated values.

[21] From the above comparison between the model calculations and the measurements during TOPSE, there is a clear indication that N$_2$O$_5$ hydrolysis on sulfate aerosols plays a very important role in controlling NO$_x$ and O$_3$ budgets in the NH troposphere during winter and spring. The effect on seasonal, latitudinal, and altitudinal patterns are consistent with the model assessments, confirming that this observed evidence is solid and significant. However, as expected, there are uncertainties in the model calculation. To further confirm this conclusion, uncertainties related to the calculations of hydrolysis of N$_2$O$_5$ on sulfate aerosol in the model will be analyzed in the following section.

2.3. Uncertainty Analysis

[22] There are uncertainties in the model in estimating the effect of the hydrolysis of N$_2$O$_5$ on NO$_x$ and O$_3$ concentrations. The major uncertainties are related to the predicted aerosol loadings and the measured heterogeneous uptake coefficient γ indicated in Equation (2). From Equation (2), we see that the reaction coefficient k$_{het}$ is a linear product of uptake coefficient γ and sulfate surface area A. Uncertainties in γ and A will produce the uncertainties in the reaction coefficient k$_{het}$, and thus in the model calculation of the effect of R-4 on NO$_x$ concentrations.

[23] The reaction of N$_2$O$_5$ on sulfate aerosol, which produces HNO3, has been measured by several groups who have found values of γ ranging from 0.02 to 0.10 [*Van Doren et al.*, 1991; *Hanson and Ravishankara*, 1992; *Fried et al.*, 1994; *George et al.*, 1994; *Hanson and Lovejoy*, 1994; *Zhang et al.*, 1995; *Robinson et al.*, 1997]. The lowest uptake coefficient is observed by *George et al.* [1994], who report values decreasing from 0.03 to 0.013 with increasing temperature. *Hu and Abbatt* [1997] measured the uptake coefficient at various atmospheric conditions. Their measurement shows that the uptake coefficient varies from 0.01 to 0.1 depending on air temperature, humidity, and aerosol composition. When temperature and humidity values are close to tropospheric conditions, the reaction coefficient is measured between 0.017 and 0.06. However, when humidity and temperature are very low (stratospheric condition), the reaction coefficient is around 0.1 which is the value widely used in stratospheric models [*Hofman and Solomon*, 1989; *Rodriguez et al.*, 1991; *Tie et al.*, 1994].

[24] The model predicted sulfate aerosol has been analyzed by *Tie et al.* [2001]. The simulated global sulfate aerosol distributions are generally in agreement with measurements. The calculated vertical profiles of sulfate aerosols agree well with the observations over North America. During TOPSE sulfate aerosol concentrations were measured and compared with the model results (see Figure 11). Figure 11 shows that the modeled sulfate aerosol is generally consistent with the measured values. Specifically, the seasonal variability is shown in both the model and observation, i.e. the concentrations of sulfate aerosol are higher in spring than in winter. As analyzed by *Tie et al.* [2001], during winter, the chemical conversion of SO$_2$ to sulfate is low (low OH and H$_2$O$_2$ concentrations), and the boundary layer ventilation is weak, leading to high SO$_2$ and low sulfate concentrations. The differences between modeled and observed sulfate aerosol concentrations are generally within a factor of 2. The ratio of 2 in mass concentrations (volume) is about the ratio of 1.6 in surface area.

[25] As shown in Equation 2, the reaction coefficient of R-4 is the product of aerosol surface area and uptake coefficient, i.e. k$_{het}$ ∝ (Aγ). Thus, to change the reaction coefficient, we can either change the uptake coefficient or
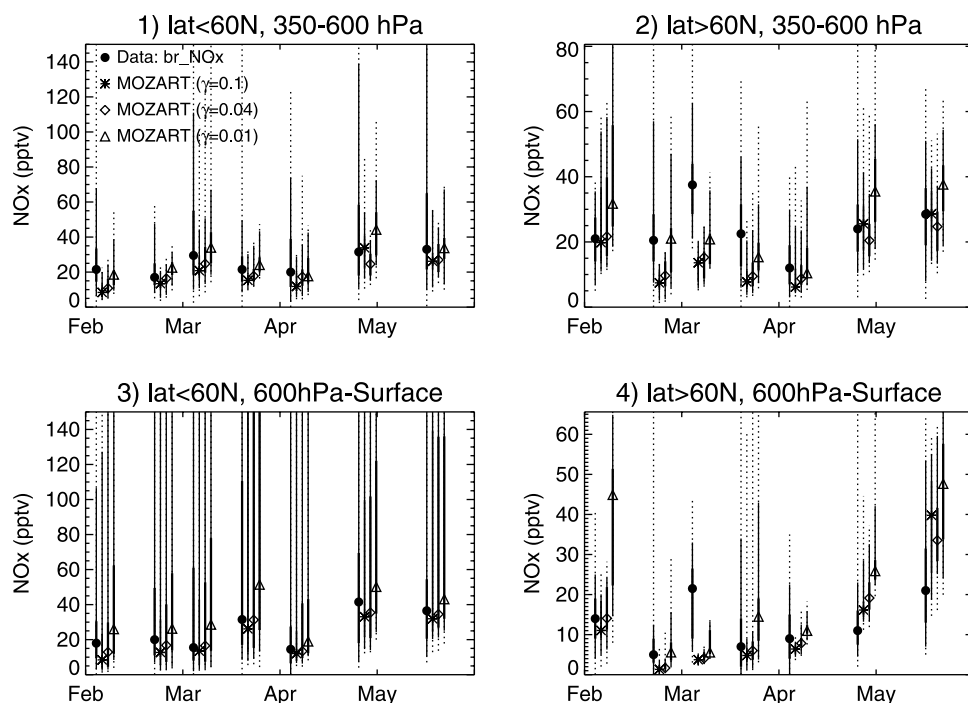
Figure 12. Comparison of the calculated to the observed NO$_x$ concentrations (pptv) during TOPSE in the following 4 different regions as in Figure 7. The black dots are the measured NO$_x$ concentrations; the asterisks are the calculated values with hydrolysis of N$_2$O$_5$ at sulfate aerosol (γ = 0.1); the diamonds are the calculated values with hydrolysis of N$_2$O$_5$ at sulfate aerosol (γ = 0.04); and the triangles are the calculated values with hydrolysis of N$_2$O$_5$ at sulfate aerosol (γ = 0.01). The symbols indicate the median values, with thick lines between 25% and 75% of the data, thin lines 5% and 95% and dashed lines between extrema.

the aerosol loadings. To reveal the impact of the uncertainties related to uptake coefficient and aerosol loadings on the model calculation, several model runs were made with the following conditions; (1) uptake coefficient = 0.1 which is the upper limit of the coefficient, (2) uptake coefficient = 0.04 which is the middle value of the coefficient, and (3) uptake coefficient = 0.01 which is the lower limit of the coefficient. As we described, the changes of the uptake coefficient can be also considered as changes in aerosol loading while the uptake coefficient is a constant. In this case, the aerosol loading is changed by a factor of 10 from condition (1) to condition (3), which fully covers the differences between the model calculation and the measurement shown in Figure 11. As indicated in Figure 2, with an upper value of uptake coefficient (γ = 0.1), the reaction of R-4 is about 11 times faster than the reaction of R-1, so that R-1 is the determining rate for the conversion of NO$_2$ to HNO$_3$. As a result, a further increase in the uptake coefficient or aerosol loading will not change the net conversion from NO$_2$ to HNO$_3$ because the conversion is limited by the slower rate of R-1. However, a further decrease in the rate of R-4 to the value that is comparable to the rate of R-1 can reduce the net conversion from NO$_2$ to HNO$_3$. As indicated in Figure 12, between the conditions (1) and (2), which imply that either uptake coefficient or aerosol loading is reduced by 4 times, the calculated NO$_x$ concentrations change slightly, indicating that with a reduction of 4 times in reaction coefficient of R-4, the conversion is still limited by the reaction of R-1. However, between the conditions (1) and (3) which imply

that the reaction coefficient of R-4 is reduced by 10 times, the calculated NO$_x$ concentrations change, indicating that in this case the rate of R-4 is comparable to the rate of R-1, and the conversion from NO$_2$ to HNO$_3$ is reduced due to the decrease in hydrolysis of N$_2$O$_5$. A similar situation is also shown in the calculated O$_3$ concentrations (see Figure 13). The averaged NO$_x$ and O$_3$ concentrations with different rates for the hydrolysis of N$_2$O$_5$ on sulfate aerosol during March TOPSE flights are summarized in Table 1. It clearly indicates that hydrolysis of N$_2$O$_5$ has a significant impact on NO$_x$ and O$_3$ concentrations during TOPSE. The uncertainties related to reaction coefficient have much smaller effects than the hydrolysis itself.

[26]   To better understand the saturation effect of hydrolysis of N$_2$O$_5$ on NO$_x$ concentrations in the troposphere, we show in Figure 14 the changes in NO$_x$ as a function of aerosol surface area. The calculations were made with a photochemical box model which included a highly detailed description for the photo-oxidation of hydrocarbons (C1–C8) in the presence of HO$_x$ and NO$_x$ [*Madronich and Calvert*, 1989]. The chemistry was recently updated to the recommendations of *Demore et al.* [1997] and *Atkinson* [1997]. The model was run over representative diurnal profiles with photolysis rate coefficients calculated using Tropospheric Ultraviolet (TUV) radiation code [*Madronich*, 1989]. Several cases were modeled for different altitudes (1–3 km vs. 6–8 km), latitudes (40–50°N vs. 58–85°N) and months (February and May). For each case, the box model was initialized with measured median values derived
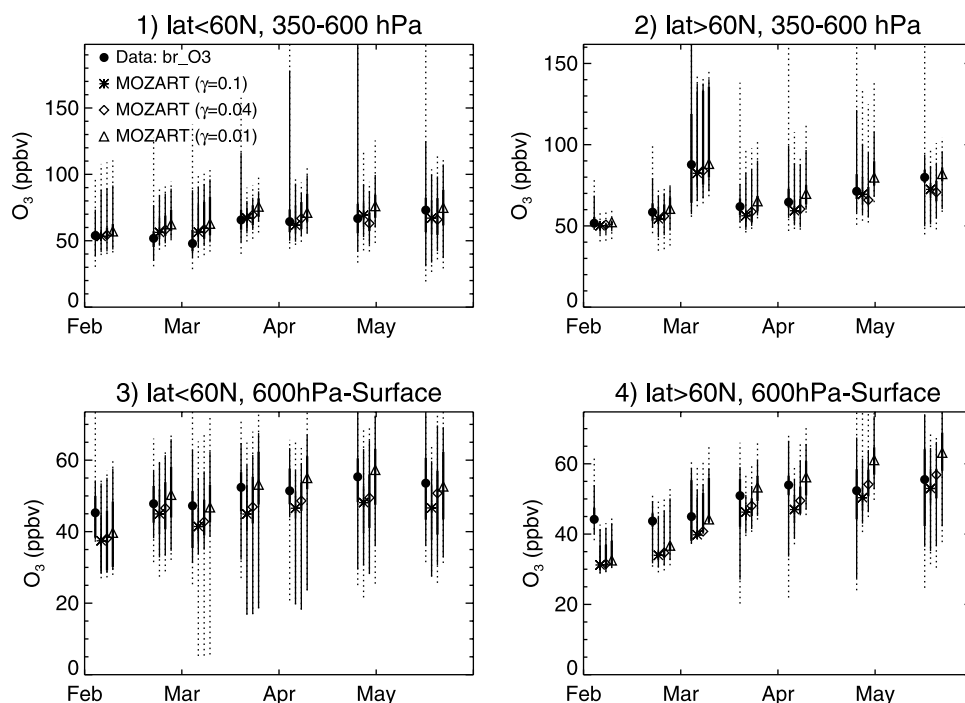
Figure 13. Same as Figure 12 except for O$_3$.

from the TOPSE aircraft data archive (with the exception of NO$_x$ which was initialized at 600 pptv for all cases). The model was run unconstrained over 6 diurnal cycles with a constant N$_2$O$_5$ uptake coefficient of 0.1. For each case, runs with varying surface areas were performed so that the point of saturation could be studied. In high latitudes (58–85°N) of the lower troposphere (1–3 km) in winter (February), hydrolysis of N$_2$O$_5$ had the greatest effect on NO$_x$ concentrations. When hydrolysis was included in the model, the NO$_x$ concentrations decreased rapidly with increases in surface areas. More than an 80% reduction in NO$_x$ was modeled when the sulfate area was above 10 μm^2/cm^3. A saturation point was reached at 10 μm^2/cm^3. In high latitudes of the middle to high troposphere (6–8 km) in winter, the effect of hydrolysis of N$_2$O$_5$ on NO$_x$ concentrations was smaller than in the lower troposphere. About 40% reduction in NO$_x$ was produced when the surface area was above 10 μm^2/cm^3. Again, a saturation point was reached at 10 μm^2/cm^3. In middle latitudes (40–50°N) of the lower troposphere in winter, the effect of hydrolysis of N$_2$O$_5$ on NO$_x$ concentrations was smaller than in the high latitudes. About 40% reduction in NO$_x$ was modeled when the sulfate area was above 50 μm^2/cm^3. A saturation point was reached when the surface area was above 50 μm^2/cm^3. In spring (May), the effect of hydrolysis of N$_2$O$_5$ on NO$_x$ concentrations was very small. The saturation point is basically the point when the reaction of NO$_2$ with O$_3$ (R-3) and the hydrolysis (R-4) are competitive. As a result, saturation depends on sulfate surface areas as well as O$_3$ and NO$_2$ concentrations. When O$_3$ and NO$_2$ concentrations are high, such as in middle latitudes of North America, saturation is reached with a higher sulfate surface area than in high latitudes. Modeled sulfate surface areas range between 10 to 30 μm^2/cm^3 in high latitudes and more than 50 μm^2/cm^3 in middle latitudes in the NH [*Tie et al.*, 2001]. Thus,

saturation is normally reached during TOPSE. For example, in high latitudes in winter, if the surface area changes from 30 μm^2/cm^3 to 10 μm^2/cm^3, only small changes in NO$_x$ concentrations will result.

[27] From the above analysis, we see that within the uncertainty range of the reaction coefficient, the model calculated NO$_x$ and O$_3$ concentrations change moderately. However, such changes are much smaller than the differences between the model runs with and without R-4 (see Figures 9a, 9b, and 12). Within some uncertainties in the uptake coefficient or aerosol loading, the TOPSE comparison provides strong evidence that hydrolysis of N$_2$O$_5$ plays an important role in controlling NO$_x$ and O$_3$ budgets.

3. Summary

[28] A comprehensive global chemical/transport/aerosol model (MOZART) is used to study the impact of hydrolysis

Table 1. Measured and Calculated NO$_x$ and O$_3$ During TOPSE in March

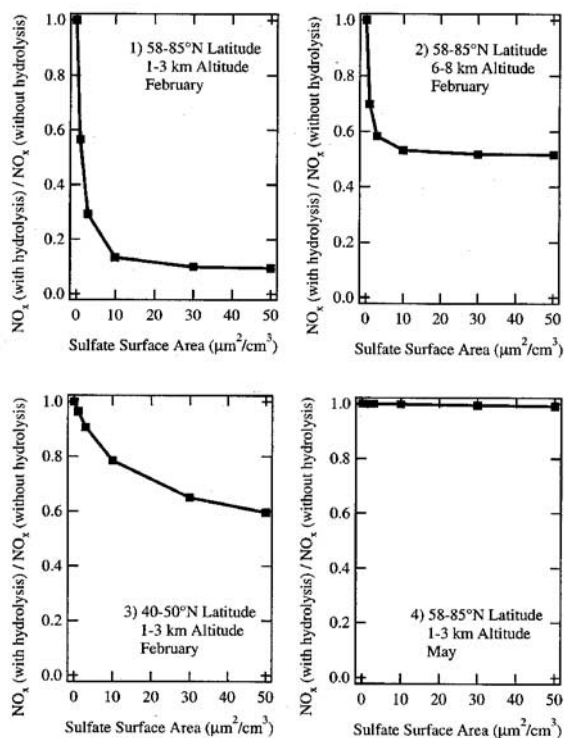|	lat < 60N 350–600 hPa	lat > 60N 350–600 hPa	lat < 60N 600 hPa-Surf	lat > 60N 600 hPa-Surf
	NO$_x$(pptv)			
Obs.	24.5	25.0	23.0	8.5
$\gamma = 0.0$	40.3	44.6	244.6	272.3
$\gamma = 0.04$	20.1	9.9	22.8	5.8
$\gamma = 0.10$	16.8	8.3	18.3	4.5
	O$_3$(ppbv)			
Obs.	59.1	63.1	50.5	50.3
$\gamma = 0.0$	83.6	84.5	65.8	72.1
$\gamma = 0.04$	65.6	60.4	45.3	47.9
$\gamma = 0.10$	62.9	58.2	43.4	46.2
Obs.	59.1	63.1	50.5	50.3

Figure 14. NO$_x$ changes for different sulfate surface areas calculated with a chemical box model for different conditions; (1) in high latitudes (58–85°N) at 1–3 km in February, (2) in high latitudes (58–85°N) at 6–8 km in February, (3) in middle latitudes (40–50°N) at 1–3 km in February, and (4) in high latitudes (58–85°N) at 1–3 km in May. An uptake coefficient for N$_2$O$_5$ hydrolysis of 0.1 was used for all simulations.

of N$_2$O$_5$ on sulfate aerosol on NO$_x$ and O$_3$ budgets. To study this impact, the MOZART model was run for different conditions (with and without the hydrolysis of N$_2$O$_5$). The model calculation shows that the globally averaged reduction of NO$_x$ due to the heterogeneous reaction on sulfate aerosols has a strong seasonal variation, with a reduction of 38 and 6% during December and June, respectively. Much more of the reduction occurs in the NH than in the SH. In the NH, the reduction of NO$_x$ is 47 and 7% during December and June, respectively. While in the SH, the reduction of NO$_x$ is 3 and 5% during December and June, respectively. Despite the strong seasonal variation of the reduction of NO$_x$, the globally averaged reduction of O$_3$ has a weak seasonal variation, with 6 and 4% during December and June, respectively. However, in December the O$_3$ reduction shows a large hemispheric asymmetry, with 8 and 2% in the NH and the SH, respectively. The model results also reveal that the maximum impact of hydrolysis of N$_2$O$_5$ on sulfate aerosol on NO$_x$ occurs at high latitudes of the NH during winter. Because the TOPSE experiment was designed to investigate the chemical and dynamic evolution of tropospheric chemical composition over the middle to high latitude continental North America during the winter/spring transition, it provided valuable data to study the impact of hydrolysis of N$_2$O$_5$ at sulfate aerosol on NO$_x$ and

O$_3$ budgets at high latitudes of the NH. The calculated results are compared with field measurements (TOPSE), and this comparison shows clear evidence that the hydrolysis of N$_2$O$_5$ on sulfate aerosol plays an important role in controlling tropospheric NO$_x$ and O$_3$ budgets at high latitudes of the Northern Hemisphere in winter and spring. The calculations indicate that without this heterogeneous reaction, the model calculated NO$_x$ concentrations are very high (300 to 600 pptv) at high latitudes of the NH in winter and early spring, which is much higher than the measured values during TOPSE (below 20 pptv). With the hydrolysis reaction, modeled NO$_x$ concentrations are close to the measured values. Several model runs using different values of the reaction coefficient of hydrolysis of N$_2$O$_5$ are conducted to study the effect of uncertainties in the model on the calculated NO$_x$ concentrations. The analysis indicates that the changes in NO$_x$ due to model uncertainties are much smaller than the impact of hydrolysis of N$_2$O$_5$ on sulfate aerosol.

References

Atkinson, R., Gas-phase tropospheric chemistry of volatile organic compounds, 1, Alkanes and alkenes, *J. Phys. Chem. Ref.*, *26*, 215–290, 1997.

Atlas, E., B. Ridley, and C. Cantrell, The Tropospheric Ozone Production About the Spring Equinox (TOPSE) Experiment: Introduction, *J. Geophys. Res*, doi:10.1029/2002JD003172, in press, 2002.

Bekki, S., and J. A. Pyle, A two-dimensional modelling study of the volcanic eruption of Mount Pinatubo, *J. Geophys. Res.*, *99*, 18,861–18,870, 1994.

Blake, D. F., and K. Kato, Latitudinal distribution of black carbon soot in the upper troposphere and lower stratosphere, *J. Geophys. Res.*, *100*, 7195–7202, 1995.

Brasseur, G., and C. Granier, Mount Pinatubo aerosols, chlorofluorocarbons, and ozone depletion, *Science*, *257*, 1239–1242, 1992.

Brasseur, G. P., D. A. Hauglustaine, S. Walter, J. F. Muller, P. Rasch, C. Granier, and X. Tie, MOZART: A global three-dimensional Chemical-Transport-Model of the atmosphere, *J. Geophys. Res.*, *103*, 28,265–28,289, 1998.

Chatfield, R., Anomalous HNO3/NOx ratio of remote tropospheric air: Conversion of nitric acid to formic acid and NOx?, *Geophys. Res. Lett.*, *21*, 2705–2708, 1994.

Demore, W. B., S. P. Sander, D. M. Golden, R. F. Hampson, M. J. Kurylo, C. J. Howard, A. R. Ravishankara, C. E. Kolb, and M. J. Molina, Chemical kinetics and photochemical data for use in stratospheric modeling, Evaluation number 12, *JPL Publ. 97-4*, NASA/Jet Propulsion Lab., Pasadena, Calif., 1997.

Dentener, F. J., and P. J. Crutzen, Reaction of N$_2$O$_5$ on tropospheric aerosols: Impact on the global distributions of NO$_x$, O$_3$, and OH, *J. Geophys. Res.*, *98*, 7149–7163, 1993.

Fahey, D. W., et al., In situ measurements constraining the role of sulfate aerosols in mid-latitude ozone depletion, *Nature*, *363*, 509–514, 1993.

Fried, A., B. E. Henry, J. G. Calvert, and M. Mozurkewich, The reaction probability of N$_2$O$_5$ with sulfuric acid aerosols at stratospheric temperatures and compositions, *J. Geophys. Res.*, *99*, 3517–3532, 1994.

George, C., J. L. Ponche, Ph. Mirabel, W. Behnke, V. Scheer, and C. Zetzsch, Study of the uptake of N$_2$O$_5$ by water and NaCl solutions, *J. Phys. Chem.*, *98*, 8780–8784, 1994.

Hanson, D. H., and A. R. Ravishankara, Investigation of the reactive and nonreactive processes involving ClONO$_2$ and HCl on water and nitric acid doped ice, *J. Phys. Chem.*, *96*, 2682–2691, 1992.

Hanson, D. H., and E. R. Lovejoy, The uptake of N$_2$O$_5$ onto small sulfuric acid particles, *Geophys. Res., Lett.*, *21*, 2401–2404, 1994.

Hauglustaine, D. A., G. P. Brasseur, S. Walters, P. J. Rasch, J. F. Muller, L. K. Emmons, and M. A. Carroll, MOZART, a global chemical transport model for ozone and related chemical tracers, Model results and evaluations, *J. Geophys. Res.*, *103*, 28,291–28,335, 1998.

Hofmann, D. J., and S. Solomon, Ozone destruction through heterogeneous chemistry following the eruption of El Chichon, *J. Geophys. Res.*, *94*, 5029–5041, 1989.

Hu, J. H., and J. P. D. Abbatt, Reaction probabilities for N$_2$O$_5$ hydrolysis on sulfate acid and ammonium sulfate aerosols at room temperature, *J. Phys. Chem. A*, *101*, 871–878, 1997.

Jacob, D. J., et al., Origin of ozone and NOx in the tropical troposphere: a photochemical analysis of aircraft observations over the South Atlantic Basin, *J. Geophys. Res.*, *101*, 24,235–24,256, 1996.

Johnston, P. V., R. L. McKenzie, J. G. Keys, and W. A. Mattews, Observations of depleted stratospheric NO$_2$ following the Pinatubo volcanic eruption, *Geophys Res. Lett.*, *19*, 211–213, 1992.

Koike, M., N. B. Jones, W. A. Mattews, P. V. Johnston, R. L. McKenzie, D. Kinnison, and J. Rodriguez, Impact of Pinatubo aerosols on the partitioning between NO$_2$ and HNO$_3$, *Geophys. Res. Lett.*, *21*, 597–600, 1994.

Lin, S. J., and R. B. Rood, Multidimensional flux-form semi-Lagrangian transport schemes, *Mon. Weather Rev.*, *124*, 2046–2070, 1996.

Madronich, S., Photodissociation in the atmosphere, 1, Actinic flux and the effect of ground reflections and clouds, *J. Geophys. Res.*, *92*, 9740–9752, 1989.

Madronich, S., and J. G. Calvert, The NCAR master chemical mechanism of the gas phase chemistry, *NCAR Tech. Rep. TN-333+STR*, Natl. Cent. for Atmos. Res., Boulder, Colo., 1989.

Muller, J.-F., and G. Brasseur, IMAGES: A three-dimensional chemical transport model of the global troposphere, *J. Geophys. Res.*, *100*, 16,445–16,490, 1995.

Perry, R. H., and D. Green, *Perry's Chemical Engineers Handbook*, pp. 3–285, McGraw-Hill, New York, 1984.

Pitari, G., and V. Rizi, An estimate of the chemical and radiative perturbation of stratospheric ozone following the eruption of Mt. Pinatubo, *J. Atmos. Sci.*, *50*, 3260–3276, 1993.

Prinn, R. G., et al., Atmospheric trends in methyl chloroform and the global average for the hydroxyl radical, *Science*, *238*, 945–950, 1987.

Rodriguez, J. M., M. K. W. Ko, and N. D. Sze, The role of heterogeneous conversion of N$_2$O$_5$ on sulfate aerosols in global ozone losses, *Nature*, *352*, 134, 1991.

Robinson, G. N., D. R. Worsnop, J. T. Jayne, C. E. Kolb, and P. Davidovits, Heterogeneous uptake of ClONO$_2$ and N$_2$O$_5$ by sulfuric acid solutions, *J. Geophys. Res.*, *102*, 3583–3601, 1997.

Schwartz, S. E., Mass-transport considerations pertinent to aqueous phase reactions of gases in liquid water clouds, in *Chemistry of Multiphase Atmospheric System*, *NATO ASI Ser., Ser. G*, edited by W. Jaeschke, Springer-Verlag, New York, 1986.

Shettle, E. P., and R. W. Fenn, Models for the aerosols of the lower atmosphere and the effects of humidity variations on their optical properties, *Publ. AFGL-TR-79-0214*, Air Force Geophys. Lab., Hanscom, Mass., 1979.

Sillman, S., J. A. Logan, and S. C. Wofsy, The sensitivity of ozone to nitrogen oxides and hydrocarbons in regional ozone episodes, *J. Geophys. Res.*, *95*, 1837–1851, 1990.

Tie, X., C.-Y. Kao, E. Mroz, R. Cicerone, F. Alyea, and D. Cunnold, Three-dimensional simulations of atmospheric methylchloroform: Effect of an ocean sink, *J. Geophys. Res.*, *97*, 20,751–20,769, 1992.

Tie, X., G. P. Brasseur, B. Briegleb, and C. Granier, Two-dimensional simulation of Pinatubo aerosol and its effect on stratospheric ozone, *J. Geophys. Res.*, *99*, 20,545–20,562, 1994.

Tie, X., G. Brasseur, L. Emmons, L. Horowitz, and D. Kinnison, Effects of aerosols on tropospheric oxidants: A global model study, *J. Geophys. Res.*, *106*, 22,931–22,964, 2001.

Van Doren, J. M., L. R. Watson, P. Davidovits, D. R. Worsnop, M. S. Zahniser, and C. E. Kolb, Uptake on N$_2$O$_5$ and HNO$_3$ by aqueous sulfuric acid droplets, *J. Phys. Chem.*, *95*, 1684–1689, 1991.

Wang, Y., J. Logan, and D. Jacob, Global simulation of tropospheric O$_3$-NOx-hydrocarbon chemistry, 2, Model evaluation and global ozone budget, *J. Geophys. Res.*, *103*, 10,727–10,755, 1998.

Wang, Y., D. J. Jacob, and J. A. Logan, Global simulation of tropospheric O$_3$-NO$_x$-hydrocarbon chemistry, 3, Model simulation, *J. Geophys. Res.*, *103*, 10,713–10,725, 1998.

Zhang, G. J., and N. A. McFarlane, Sensitivity of climate simulations to the parameterization of cumulus convection in the Canadian Climate Center General circulation model, *Atmos. Ocean*, *33*, 407–446, 1995.

Zhang, R. Y., M. T. Leu, and L. F. Keyser, Sulfuric acid monohydrate: Formation and heterogeneous chemistry in the stratosphere, *J. Geophys. Res.*, *100*, 18,845–18,854, 1995.

————————————

E. Atlas, L. Emmons, P. Hess, A. Klonecki, S. Madronich, B. Ridley, C. Stround, and X. Tie, National Center for Atmospheric Research, 1850 Table Mesa Drive, Boulder, CO 80307, USA. (xxtie@ucar.edu)

L. Horowitz, NOAA/GFDL, Princeton University, POB 308, Princeton, NJ 08542, USA.

G. Brasseur, Max-Planck Inst Meteorologie, Bundestrasse 55, Hamburg, 20146 Germany.

J. Dibb and R. Talbot, Institute for the Study of Earth, Oceans, and Space, University of New Hampshire, Morse Hall, 39 College Road, Durham, NH 03824, USA.